On the Integration of Grassmannian Constellations into LTE Networks: a Link-level Performance Study

Jorge Cabrejas, David Martín-Sacristán, Sandra Roger, Daniel Calabuig and Jose F. Monserrat

iTEAM Research Institute

Universitat Politècnica de València (UPV)

Camino de Vera S/N, 46022, Valencia, Spain

{jorcabpe, damargan, sanrova, dacaso, jomondel}@iteam.upv.es

Abstract—**This paper presents Grassmannian signaling as a transmission scheme that can be integrated in Long Term Evolution (LTE) to support higher user speeds and to increase the throughput achievable in the high Signal to Noise Ratio (SNR) regime. This signaling is compared, under realistic channel assumptions, with the diversity transmission modes standardized in LTE, in particular, Space-Frequency Block Coding and Frequency-Switched Transmit Diversity for two and four transmit antennas, respectively. In high-speed scenarios, and even with high antenna correlation, Grassmannian signaling outperforms the LTE diversity transmission modes starting from four transmit antennas. Furthermore, in the high SNR regime, Grassmannian signaling can increase the link data rate up to 10% and 15% for two and four antennas, respectively.**

Index Terms—**Non-coherent communications, Grassmannian signaling, transmit diversity, LTE, OFDM, channel correlation.**

I. INTRODUCTION

Mobile communication systems have been traditionally based on coherent reception, for which a set of pilot sequences is sent to the receiver to estimate the channel and perform coherent data detection. However, these traditional systems have two main practical drawbacks, namely, pilot contamination and loss in spectral efficiency. Furthermore, both drawbacks are aggravated when increasing the number of transmit antennas [1], [2].

Pilot contamination arises when a transmitter sends pilot sequences in the same resources as nearby transmitters, thus polluting the channel estimate of other receivers, and hence, reducing the system capacity [1]. With respect to the loss in spectral efficiency, coherent systems must dedicate a significant portion of the available resources to pilot transmission to estimate the channel with sufficient accuracy [3]. This implies a certain efficiency loss since these resources could have been used to transmit data instead. Therefore, there is a trade-off between channel estimation accuracy and availability of resources for data transmission. In the particular case of Multiple Input Multiple Output (MIMO) LTE modes, for two transmit antennas, about 10% of resources are reserved for pilots, a percentage that ensures acceptable performance even for high-speed users (up to 500 km/h) [2], [4]. For four transmit antennas, although 20% of the resources should be reserved to maintain the same channel estimation accuracy, only around 15% of resources are allocated to pilot signals, thus reducing the channel estimation accuracy compared to

the two antenna setup. Consequently, this pilot arrangement assumes that the MIMO transmission modes with four transmit antennas will be only used for low-speed users, which entails an important limitation to fulfill one of the key goals of fifth generation (5G) mobile systems, that is, to provide mobile broadband services in vehicular environments with a high number of transmit antennas [5].

All the aforementioned drawbacks are even aggravated when increasing the number of transmit antennas, as several pilot sequences should be transmitted for adequate channel estimation from every antenna. As a consequence, the pilot contamination is intensified and the available resources for data transmission are strongly reduced.

The main problems of coherent training-based communication motivated the increasing research on non-coherent MIMO communication techniques, which are able to perform data detection without any knowledge of the channel coefficients at the receiver side and, thus, they do no longer require the transmission of pilots [6–11]. Non-coherent MIMO communication schemes specifically designed for block-fading channels were proposed in [6], [7]. The authors in [8] showed that the optimal capacity-achieving input signals are unitary matrices isotropically distributed on the compact Grassmann manifold. Some Grassmannian Constellations (GCs) that mimic the optimal capacity-achieving input signals can be found in [9]. In [10], the use of these constellations was generalized from the block-fading channel, traditionally invariant in time, to a block-fading channel, invariant not only in time but also in frequency. In [11], authors extended the use of GCs in a multi-user downlink communication and proposed a suboptimum detection scheme of linear complexity whose performance provided, in some cases, gain in the user rates with respect to the single-user detection.

Although the design of GCs is gaining momentum, so far they have been mainly studied from a theoretical point of view and their performance in realistic mobile systems is, to the best of the authors' knowledge, still unknown. First, GCs are designed for a block-fading Rayleigh channel, i.e., the channel coefficients are invariant during the block length, in a given bandwidth, and are drawn independently for the subsequent block. However, in practical systems, temporal correlation between the channel coefficients due to the user mobility and frequency selectivity caused by the multi-path channel break

this assumption independently of how the GCs are mapped in the time and frequency domains. It is also worth noting that GCs do not operate optimally with correlated antennas and experience a loss of coding gain [12].

In [13], a subset of well-known non-coherent techniques, including GCs, were compared with several state-of-art training-based coherent schemes over temporally-correlated Rayleigh-fading MIMO channels in a simplified simulation setup. Such comparison showed that non-coherent schemes are meaningful alternatives to training-based communication, especially as the number of transmit antennas increases. In particular, for more than two transmit antennas, non-coherent communication provided a certain advantage in medium to high mobility scenarios. Guided by the results of [13] and motivated by the lack of performance results including GCs in practical systems which feature realistic channels, this paper investigates, by means of link-level simulations, the integration of Grassmannian signaling into the LTE standard and provides a fair comparison with LTE transmit diversity modes, which are based on coherent space-frequency modulation.

The rest of the paper is organized as follows. Section II presents the system model. Section III presents the primary characteristics of the LTE transmit diversity modes and the Grassmannian signaling. Section IV describes the simulation setup and assumptions considered in this work. Results are presented in Section V. Finally, conclusions are described in Section VI.

II. SYSTEM MODEL

We consider a downlink Orthogonal Frequency Division Multiplexing (OFDM) single-user system with M antennas at the Base Station (BS) and N antennas at the User Equipment (UE), leading to an $M \times N$ MIMO system. The transmitter sends information blocks of K bits over T channel uses (in the LTE terminology, a channel use is composed of a subcarrier during an OFDM symbol) and M transmit antennas, thus, the resulting transmission rate is $R = K/T$ bits per channel use (bpcu). Each data block consists of a $T \times M$ complex matrix

$$\mathbf{X} = [\mathbf{x}_1, \mathbf{x}_2, \ldots, \mathbf{x}_t, \ldots, \mathbf{x}_T]^\mathsf{T},$$

where $\mathbf{x}_t \in \mathbb{C}^{M \times 1}$, is the signal transmitted by the M antennas at channel use t with $\mathbb{E}\left[\|\mathbf{x}_t\|^2\right] = 1$, $t \in \{1, \ldots, T\}$. The superscript T and $\mathbb{E}[\cdot]$ stand for matrix transposition and expectation operation, respectively. After T channel uses, the receiver processes the $T \times N$ matrix $\mathbf{Y} = [\mathbf{y}_1, \mathbf{y}_2, \ldots, \mathbf{y}_t, \ldots, \mathbf{y}_T]^\mathsf{T}$ for demodulation, where

$$\mathbf{y}_t^\mathsf{T} = \sqrt{\frac{\rho N T}{\mathrm{Tr}\left(\mathbf{\Gamma_H}\mathbf{\Gamma_X}\right)}} \mathbf{x}_t^\mathsf{T}\mathbf{H}_t + \mathbf{z}_t^\mathsf{T} \tag{1}$$

is the complex vector received at channel use t, $\mathbf{z}_t \in \mathbb{C}^{N \times 1}$ is the Additive White Gaussian Noise (AWGN) with zero-mean and unit-variance, ρ is the SNR, $\mathbf{\Gamma_X} = \mathbb{E}\left[\mathbf{X}^\dagger\mathbf{X}\right]$ is the signal covariance matrix, which equals the identity matrix for all transmission schemes addressed in this paper, the superscript $\dagger$ stands for the transpose conjugate operation,

$\mathbf{\Gamma_H} = \mathbb{E}\left[\mathbf{H}_t\mathbf{H}_t^\dagger\right]$ is the channel covariance matrix, and $\mathrm{Tr}\left(\cdot\right)$ is the trace operator. The MIMO channel $\mathbf{H}_t \in \mathbb{C}^{M \times N}$ is assumed to have zero-mean complex Gaussian entries with channel covariance $\mathbf{R} = \mathbb{E}\left[\mathrm{vec}(\mathbf{H}_t)\mathrm{vec}(\mathbf{H}_t)^\dagger\right]$. The operation $\mathrm{vec}(\mathbf{H}_t)$ denotes the $MN \times 1$ vector obtained by stacking columns of $\mathbf{H}_t$. Considering the Kronecker model and assuming the independence of the spatial correlation matrices at the transmitter and the receiver [14], $\mathbf{R}$ can be represented by

$$\mathbf{R} = \mathbf{R}^{Rx} \otimes \mathbf{R}^{Tx}, \tag{2}$$

where $\otimes$ denotes the Kronecker product, and $\mathbf{R}^{Tx}$ and $\mathbf{R}^{Rx}$ denote the channel transmit and receive correlation matrices, respectively, whose expressions are as follows [15]:

$$\mathbf{R}^{Tx} = \frac{\mathbb{E}\left[\mathbf{H}_t\mathbf{H}_t^\dagger\right]}{\mathrm{Tr}\left[\mathbf{R}^{Rx}\right]}, \tag{3}$$

$$\mathbf{R}^{Rx} = \frac{\mathbb{E}\left[\mathbf{H}_t^\dagger\mathbf{H}_t\right]}{\mathrm{Tr}\left[\mathbf{R}^{Tx}\right]}. \tag{4}$$

The multipath propagation conditions of the MIMO channel are implemented by a tapped delay-line model, characterized by a given Power Delay Profile (PDP) [16]. The channel variability is modeled with the classical spectrum shape and a maximum Doppler frequency $f_d = v f_c/c$, where v is the speed of the UE, f_c is the carrier frequency and $c = 3 \cdot 10^8$ m/s is the speed of light [17].

III. TRANSMISSION SCHEMES

This section describes the transmission schemes compared in this paper and discusses their convenience under realistic channel assumptions.

A. LTE diversity schemes

Transmit diversity schemes belong to the group of techniques that do not require the acquisition of channel state information at the transmitter side. For this reason, these schemes are generally used when there is no uplink feedback for channel estimation or when the feedback is not sufficiently accurate, e.g., where the channel variations cannot be tracked due to, for instance, user mobility. For $M = 2$, the LTE transmit diversity mode is known as Space-Frequency Block Coding (SFBC) and is based on the Alamouti code, which is transmitted in two channel uses according to the following matrix:

$$\mathbf{X} = \begin{bmatrix} s_1 & -s_2^* \\ s_2 & s_1^* \end{bmatrix},$$

where the symbols s_i, $i = 1, 2$, are taken from a Quadrature Amplitude Modulation (QAM) constellation Ω of size $|\Omega|$ and hence carry $\log_2(|\Omega|)$ code bits each. The fundamental characteristic of this code is that the transmitted matrix columns are orthogonal and this allows easy decoding at the receiver. In order to achieve Maximum Likelihood (ML) decoding performance using linear processing, the channel must be constant across two consecutive channel uses.

For $M = 4$, the LTE transmit diversity mode is called Frequency-Switched Transmit Diversity (FSTD) and it requires four channel uses to transmit the following matrix:

$$\mathbf{X} = \begin{bmatrix} s_1 & 0 & -s_2^* & 0 \\ s_2 & 0 & s_1^* & 0 \\ 0 & s_3 & 0 & -s_4^* \\ 0 & s_4 & 0 & s_3^* \end{bmatrix},$$

where the symbols s_i, $i = 1, 2, 3, 4$, are also taken from a QAM constellation. In this setup, two SFBC matrices are transmitted on independent subcarriers and antennas. The mapping of symbols to transmitter antennas (columns) implies that each pair of symbols is transmitted using one of the first two antennas and one of the second two antennas (for instance, the first pair of symbols is transmitted using antennas 1 and 3) between pairs of antenna ports. This design is due to the fact that the density of Reference Signals (RSs) on the third and fourth antenna is half of the first and second antenna ports. This way, the transmission avoids concentrating the less reliable channel estimates in just one of the two SFBC matrices [2].

B. Grassmannian signaling

In a MIMO system operating over a block-fading channel of length T channel uses, the generic input signals $\mathbf{X}$ that attain rates approaching the channel capacity can be represented as the product of a $T \times M$ isotropically distributed unitary matrix $\mathbf{\Phi}$ and a diagonal $M \times M$ matrix $\mathbf{V}$ with real nonnegative values [6]. Note that a unitary matrix obeys $\mathbf{\Phi}\mathbf{\Phi}^\dagger = \mathbf{I}_M$ and is isotropically distributed when its distribution is invariable when the matrix is left-multiplied by any $T \times T$ deterministic unitary matrix [6]. In [7], it was shown that, for either $T \gg M$, or at high SNR and $T > M$, the input signal can be reduced to $\mathbf{X} = \mathbf{\Phi}$, being $\mathbf{V} = \mathbf{I}_M$. In [7], this modulation was categorized as Unitary Space-Time Modulation (USTM).

The results in [6], [7] motivated the design of isotropically distributed unitary matrices on the so-called Grassmann manifold. The idea behind this approach is based on the observation that, at high SNR, when the $T \times M$ input signal matrix $\mathbf{X}$ is passed through a complex MIMO channel, the columns of the received matrix $\mathbf{Y}$ are linear combinations of the columns of $\mathbf{X}$. Due to this, the subspace spanned by the columns of $\mathbf{X}$ and $\mathbf{Y}$ is the same. Therefore, the transmitter only has to map the transmitted data to subspaces separated as much as possible. For instance, in [9], the design criterion is based on selecting distant subspaces to minimize the error probability. Figure 1 shows an exemplary GC composed of four different directions in a plane, which can be represented by four 2×1 matrices, i.e. four one-dimensional subspaces in a two-dimensional space. In [10], it was shown that GCs can achieve optimum performance when the rows (i.e., channel uses) of the input matrix $\mathbf{X}$ are mapped in time, frequency, or in a combination of both, as long as the channel has a flat response within the considered block. In this work, we will assume the use of GCs for space-frequency modulation, to allow for a fair comparison with the transmit diversity modes of LTE.
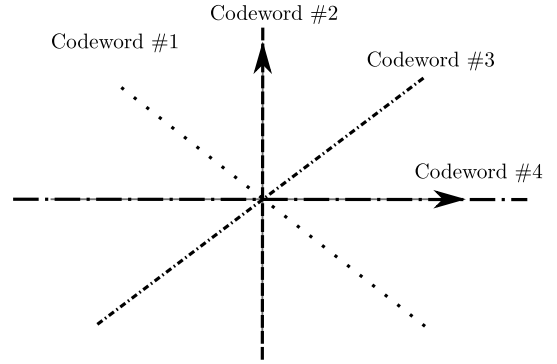

Fig. 1. Exemplary Grassmannian constellation for $M = 1$ antenna, $T = 2$ channel uses: 4 different directions in a plane.

The particular linear combination of the input signal matrix columns is not detectable by a receiver without channel knowledge. However, the M-dimensional linear subspace spanned by this basis can be indeed detected by using a Generalized Likelihood Receiver Test (GLRT) [18]. The GLRT criterion projects the received signal on the different subspaces that compose the GC. Then, it calculates the energies of all the projections and selects the projection that maximizes the energy as follows:

$$\hat{\mathbf{X}} = \arg\max_{\mathbf{S} \in \Psi} \mathrm{Tr}\left(\mathbf{Y}^\mathsf{H}\mathbf{S}\mathbf{S}^\mathsf{H}\mathbf{Y}\right), \tag{5}$$

where Ψ is the set of matrices in the GC. From the perspective of average symbol error probability minimization, in general, the GLRT provides a suboptimal result compared to the ML criterion. However, for the case of unitary constellations assumed in this work, GLRT offers the same performance as ML detection [18].

An exemplary procedure for transmission and detection using a GC is described next. Figure 2 shows the block diagram of a non-coherent transceiver, which uses $M = 1$ antenna, $T = 2$ channel uses, and the GC of Figure 1. First of all, the information bits to be transmitted are mapped to Codeword #3 through the matrix $\mathbf{X}$, where x_1 is sent in channel use 1 and x_2 is sent in channel use 2 (see Figure 2). After the codeword is transmitted, its underlying basis (the dark arrow in the subspace) is transformed by the channel, but it remains in the same subspace as the original codeword. Note that, in this example, the channel h is the same for the two channel uses. Although the non-coherent receiver cannot detect the particular transformation caused by the channel, at high SNR, it can indeed identify the subspace spanned by this basis. Therefore, the transmitted information can be recovered without any knowledge of the channel at the receiver side.

IV. SIMULATION SETUP

In order to evaluate the behavior of the Grassmannian signaling, simulations have been conducted in an LTE link-level simulator calibrated in the European project Wireless
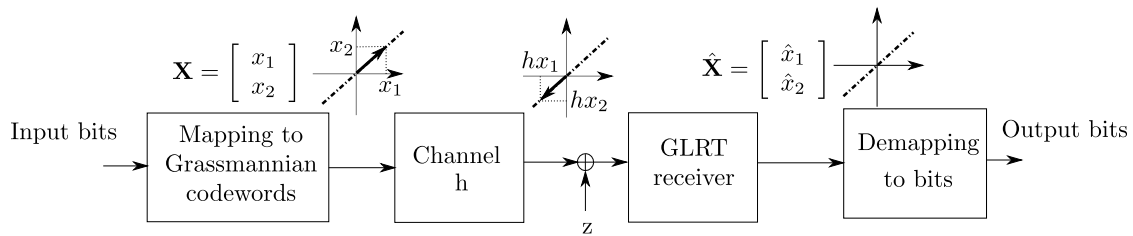
Fig. 2. Block diagram of a non-coherent transceiver with $M = 1$ antenna and $T = 2$ channel uses.

Low		Medium		High	
α	β	α	β	α	β
0	0	0.3	0.9	0.9	0.9

World Initiative New Radio + (WINNER+) [19]. The simulation was run for six resource blocks (1.4 MHz) over the Extended Vehicular A (EVA) Third Generation Partnership Project (3GPP) channel at $f_c = 2.6$ GHz [16]. We neither assumed channel coding nor retransmissions of erroneous subframes.

Both coherent LTE baselines consider a channel estimator based on Wiener filtering in both frequency and time domains [20]. This channel estimator knows the frequency and time correlation of the channel, as well as the noise power, and uses the standardized LTE RS for channel estimation. At the receiver side, the coherent schemes decode the received signal with a Minimum Mean Square Error (MMSE) detector. Conversely, the transmission based on Grassmannian signaling does not rely on pilots and sends only data blocks using T subcarriers. We here use $T = 6$ for two transmit antennas and $T = 8$ for four transmit antennas, with $R = 1$ and $R = 2$ bpcu, and only the performance of the best scheme is represented at each SNR.

The antenna correlation matrices considered at the BS for two and four antennas are:

$$\mathbf{R}^{Tx} = \begin{pmatrix} 1 & \alpha \\ \alpha^* & 1 \end{pmatrix}, \tag{6}$$

$$\mathbf{R}^{Tx} = \begin{pmatrix} 1 & \alpha^{1/9} & \alpha^{4/9} & \alpha \\ \alpha^{1/9*} & 1 & \alpha^{1/9} & \alpha^{4/9} \\ \alpha^{4/9*} & \alpha^{1/9*} & 1 & \alpha^{1/9} \\ \alpha^* & \alpha^{4/9*} & \alpha^{1/9*} & 1 \end{pmatrix}. \tag{7}$$

The correlation matrices at the UE for two and four antennas are:

$$\mathbf{R}^{Rx} = \begin{pmatrix} 1 & \beta \\ \beta^* & 1 \end{pmatrix}, \tag{8}$$

$$\mathbf{R}^{Rx} = \begin{pmatrix} 1 & \beta^{1/9} & \beta^{4/9} & \beta \\ \beta^{1/9*} & 1 & \beta^{1/9} & \beta^{4/9} \\ \beta^{4/9*} & \beta^{1/9*} & 1 & \beta^{1/9} \\ \beta^* & \beta^{4/9*} & \beta^{1/9*} & 1 \end{pmatrix}. \tag{9}$$

In Table I, the parameters α and β set the correlation level (low, medium, and high) following the 3GPP recommendation [16]. Note that, according to 3GPP, medium antenna correlation implies a higher correlation at the UE than at the BS. In addition, low correlation implies having totally uncorrelated antennas at both communication sides.

V. RESULTS

In this section, the perfomance of Grassmannian signaling and the diversity LTE modes in 2×2 and 4×4 MIMO setups is compared. In this assessment, realistic channel assumptions regarding user mobility and antenna correlation have been made. In the conducted simulations, a range of speed from 50 to 350 km/h with steps of 50 km/h was considered. However, for the sake of clarity, the figures of this section consider a subset of those speeds. Figures 3 and 4 show the performance comparison in 2×2 and 4×4 MIMO setups with uncorrelated antennas, considering the EVA channel model. Focusing on the 2×2 setup, Figure 3 first shows that Grassmannian signaling is quite robust to mobility, since the performance at different UE speeds is very similar. However, the SFBC scheme presents a higher variability with the UE speed, due to its dependence on an accurate channel estimation at the receiver side. Despite the latter result, SFBC still outperforms the Grassmannian signaling in all cases but at high SNR, where the non-coherent scheme can transmit approximately 10% more data than the SFBC scheme by saving the transmission of pilots.

Figure 4 shows the results for the 4×4 setup. It can be observed that, in this case, Grassmannian signaling is even more robust to mobility than in the 2×2 case. Conversely, the FSTD scheme is dramatically degraded by the user speed. In particular, this degradation starts to be very significant for speed values higher than 150 km/h. The main reason for the FSTD increased degradation is that two out of the four antennas of the LTE system are using poorer channel estimates, as these antennas are only assigned 50% of the pilot symbols in comparison to the other two antennas. Note also that, at high SNR, Grassmannian signaling obtains 15% more data rate than the FSTD scheme. As a result, Grassmannian signaling is a promising technique in high-speed scenarios with a high-enough number of transmit antennas. Indeed, in these cases, the removal of pilots entails an important increase of resources available for data transmission, together with a very low performance degradation with users' mobility.

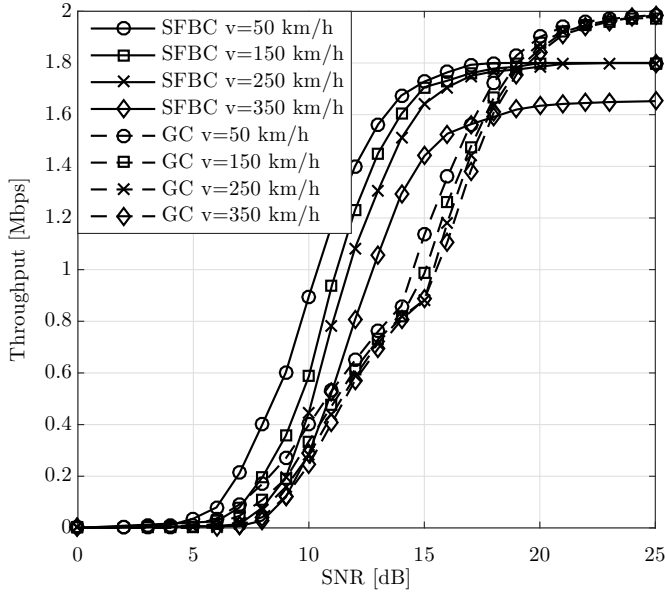In order to complete the performance analysis under real-

Fig. 3. Performance comparison among coherent and non-coherent schemes with uncorrelated antenna correlations in a 2×2 setup.
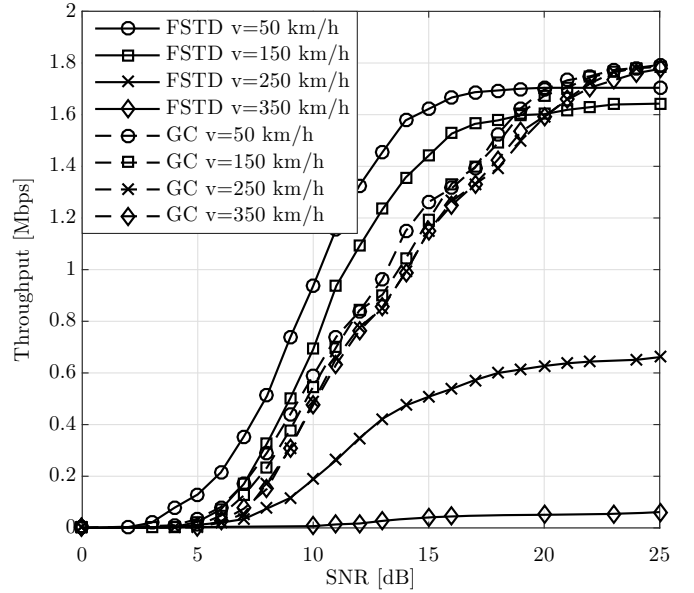

Fig. 5. Performance comparison among coherent and non-coherent schemes with medium antenna correlations in a 4×4 setup.
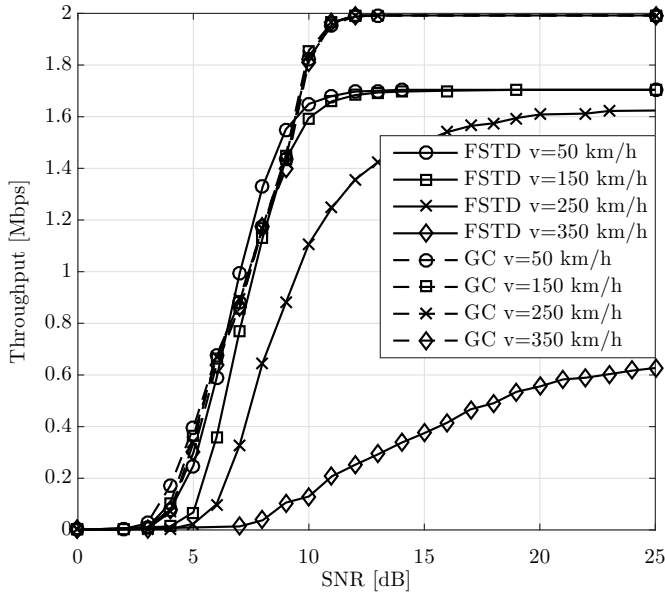

Fig. 4. Performance comparison among coherent and non-coherent schemes with uncorrelated antenna correlations in a 4×4 setup.
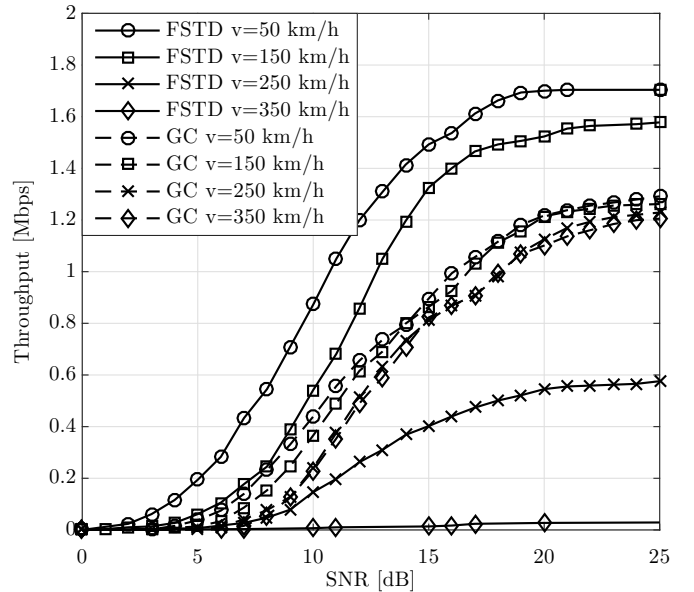

Fig. 6. Performance comparison among coherent and non-coherent schemes with high antenna correlations in a 4×4 setup.

istic conditions, we incorporated the effect of spatial antenna correlation within the 4×4 setup. Figures 5 and 6 show the obtained throughput for medium and high antenna correlation, respectively. It can be observed that antenna correlation affects both coherent and non-coherent schemes severely, but more specially Grassmannian signaling. Nevertheless, at high-speeds, Grassmannian signaling has superior performance than FSTD, due to the detrimental effect that the low temporal channel correlation has over the channel estimation. To further

illustrate this result, we set an objective throughput of 1 Mbps and analyzed the minimum speed from which Grassmannian signaling outperforms FSTD for different levels of correlation. Table II shows that this minimum value increases as the antenna correlation augments, since Grassmannian signaling relies on uncorrelated antennas. For medium and high correlations, we found that the minimum speeds correspond to those in motorways or high-speed trains. Overall, Grassmannian signaling has been shown to be especially affected by antenna

correlation and not that much by user mobility, while LTE diversity modes are more sensitive to temporal correlation, mostly when increasing the number of antennas.

TABLE II
MINIMUM USER SPEED FROM WHICH GRASSMANNIAN SIGNALING
OUTPERFORMS FSTD.

Correlation	$\mathbf{v_{min}}(km/h)$
Low	~ 100
Medium	~ 175
High	~ 225

VI. CONCLUSIONS

In this paper, a performance comparison among coherent and non-coherent communication schemes under practical channel conditions has been carried out. In particular, this paper has investigated the integration of Grassmannian signaling into an LTE-like system, by analyzing the impact of user mobility and antenna correlation using an LTE link-level simulator fully compliant with the standard. The performance of GCs have been compared with the LTE transmit diversity baselines, SFBC and FSTD, for two and four transmit antennas, respectively. This paper has compared the Grassmannian constellation with SFBC, for two antennas, and with FSTD, for four antennas. Results point out that Grassmannian signaling is a promising technique mostly for transmission in vehicular scenarios and when the number of antennas is sufficiently high. Even with only four antennas, it has been shown that the channel variability in time strongly degrades the channel estimation used in the LTE system, which makes Grassmannian signaling outperform the coherent schemes from a certain user speed, even with high antenna correlation. However, results also show that this antenna correlation affects more severely the Grassmannian signaling scheme, which further motivates the interest in focusing on vehicular communications where a massive number of antennas can be placed over a vehicle, while ensuring low correlation among them.

ACKNOWLEDGEMENT

REFERENCES

[1] O. Elijah, C. Y. Leow, T. A. Rahman, S. Nunoo, and S. Z. Iliya, "A Comprehensive Survey of Pilot Contamination in Massive MIMO-5G System," *IEEE Communications & Surveys Tutorials*, vol. 18, no. 2, pp. 905–923, 2016.

[2] S. Sesia, I. Toufik, and M. Baker, *LTE – The UMTS Long Term Evolution From Theory to Practice*. UK: John Wiley, 2011.

[3] B. Hassibi and B. M. Hochwald, "How much training is needed in multiple-antenna wireless links?" *IEEE Transactions on Information Theory*, vol. 49, no. 2, pp. 951–963, 2003.

[4] 3GPP, "TS 36.211: Physical channels and modulation (Release 12)," 2015.

[5] J. F. Monserrat, G. Mange, V. Braun, H. Tullberg, G. Zimmermann, and Ö. Bulakci, "METIS research advances towards the 5G mobile and wireless system definition," *EURASIP Journal on Wireless Communications and Networking*, vol. 2015, no. 1, pp. 1–16, 2015.

[6] T. L. Marzetta and B. M. Hochwald, "Capacity of a mobile multiple-antenna communication link in Rayleigh flat fading," *IEEE Transactions on Information Theory*, vol. 45, pp. 139–157, 1999.

[7] B. M. Hochwald and T. L. Marzetta, "Unitary space-time modulation for multiple-antenna communications in Rayleigh flat fading," *IEEE Transactions on Information Theory*, vol. 46, no. 2, pp. 543–564, 2000.

[8] L. Zheng and D. N. C. Tse, "Communication on the Grassmann manifold: a geometric approach to the non-coherent multiple-antenna channel," *IEEE Transactions on Information Theory*, vol. 48, no. 2, pp. 359–383, 2002.

[9] R. H. Gohary and T. N. Davidson, "Non-coherent MIMO communication: Grassmannian constellations and efficient detection," *IEEE Transactions on Information Theory*, vol. 55, no. 3, pp. 1176–1205, 2009.

[10] Y. M. M. Fouad, R. H. Gohary, J. Cabrejas, H. Yanikomeroglu, D. Calabuig, S. Roger, and J. F. Monserrat, "Time-Frequency Grassmannian Signalling for MIMO Multi-Channel-Frequency-Flat Systems," *IEEE Communications Letters*, vol. 19, no. 3, pp. 475–478, 2015.

[11] S. Roger, D. Calabuig, J. Cabrejas, and J. F. Monserrat, "Multi-user non-coherent detection for downlink MIMO communication," *IEEE Signal Processing Letters*, vol. 21, no. 10, pp. 1225–1229, 2014.

[12] M. Hajiaghayi and C. Tellambura, "Antenna selection for unitary space-time modulation over correlated Rayleigh channels," in *IEEE International Conference on Communications*, 2008, pp. 3824–3828.

[13] J. Cabrejas, S. Roger, D. Calabuig, Y. M. M. Fouad, R. H. Gohary, J. F. Monserrat, and H. Yanikomeroglu, "Non-Coherent Open-loop MIMO Communications Over Temporally-Correlated Channels," *IEEE Access*, vol. 4, pp. 6161–6170, 2016.

[14] J. Kermoal, L. Schumacher, K. Pedersen, P. Mogensen, and F. Frederiksen, "A stochastic MIMO radio channel model with experimental validation," *IEEE Journal on Selected Areas in Communications*, vol. 20, no. 6, pp. 1211–1226, 2002.

[15] N. Shariati and M. Bengtsson, "How far from Kronecker can a MIMO channel be? Does it matter?" in *17th European Wireless 2011 - Sustainable Wireless Technologies*, 2011, pp. 1–7.

[16] 3GPP, "TS 36.101 User Equipment (UE) radio transmission and reception (Release 12)," 2014.

[17] Y. R. Zheng and C. Xiao, "Improved models for the generation of multiple uncorrelated Rayleigh fading waveforms," *IEEE Communications Letters*, vol. 6, no. 6, pp. 256–258, 2002.

[18] M. Beko, J. Xavier, and V. Barroso, "Noncoherent Communication in Multiple-Antenna Systems: Receiver Design and Codebook Construction," *IEEE Transactions on Signal Processing*, vol. 55, no. 12, pp. 5703–5715, 2007.

[19] K. Safjan, V. D'Amico, D. Bultmann, D. Martín-Sacristán, A. Saadani, and H. Schoneich, "Assessing 3GPP LTE-advanced as IMT-advanced technology: the WINNER+ evaluation group approach," *IEEE Communications Magazine*, vol. 49, no. 2, pp. 92–100, 2011.

[20] D. Martín-Sacristán, J. Cabrejas, D. Calabuig, and J. F. Monserrat, "MAC layer performance of different channel estimation techniques in UTRAN LTE downlink," in *IEEE Vehicular Technology Conference*, 2009, pp. 1–5.